The torus parametrization of quasiperiodic LI-classes

1997 J. Phys. A: Math. Gen. 30 3029

(http://iopscience.iop.org/0305-4470/30/9/016)

J. Phys. A: Math. Gen. **30** (1997) 3029–3056. Printed in the UK PII: S0305-4470(97)77051-3

The torus parametrization of quasiperiodic LI-classes

Michael Baake†, Joachim Hermisson† and Peter A B Pleasants‡§

† Institut für Theoretische Physik, Universität Tübingen, Auf der Morgenstelle 14, D-72076 Tübingen, Germany

‡ Department of Mathematics, Macquarie University, Sydney, NSW 2109, Australia

Received 9 August 1996

Abstract. The torus parametrization of quasiperiodic local isomorphism classes is introduced and used to determine the number of elements in such a class with special symmetries or inflation properties. The method is explained in an illustrative fashion for some widely used tiling classes with golden mean rescaling, namely for the Fibonacci chain (one-dimensional), the triangle and Penrose patterns (two-dimensional) and for Kramer's and Danzer's icosahedral tilings (three-dimensional). We obtain a rather complete picture of the orbit structure within these classes, and also discuss various general results.

1. Introduction

Given a pattern, $\mathcal{P}$, in $\mathbb{R}^n$, one defines its *local isomorphism class* (LI-class for short) to be the set of all patterns $\mathcal{P}'$ locally indistinguishable from $\mathcal{P}$ in the sense that arbitrarily large parts or patches of $\mathcal{P}$ also appear in $\mathcal{P}'$ and vice versa‖. For the comparison of patches we allow only translations, not general motions, see [5, 17] for details. (In [21, 17, 22] LI-classes are called *species*.) Two standard examples of patterns are Delone point sets and tilings.

When $\mathcal{P}$ is *crystallographic* (i.e. its periods span $\mathbb{R}^n$), its LI-class is trivial, consisting only of $\mathcal{P}$ and its translates. For repetitive but non-crystallographic $\mathcal{P}$, however, the LI-class has a much richer structure and contains *uncountably many* (in fact, $2^{\aleph_0}$) translation classes [25, 7]. This makes such classes more complicated—and interesting—so good tools are needed to handle them.

Even in the crystallographic case the LI-class has an attractive topological structure: since the translate $\mathcal{P}+\ell$ is identical with $\mathcal{P}$ for any ℓ in the lattice, Λ, of periods of $\mathcal{P}$, the LI-class is in one-to-one correspondence with points of a fundamental domain of Λ which (on identifying opposite facets) is an n-dimensional torus $\mathbb{T}^n$. With a natural topology [17, 15] on the set of patterns, this one-to-one correspondence is even topological.

The key to parametrizing LI-classes of quasicrystallographic patterns is to remember that such patterns can be described as sections through crystallographic ones of higher dimensions (for which there is a unique minimal value [25, 2]). The LI-class of the quasicrystallographic pattern is then parametrized by the points of the fundamental domain

§ Present address: Department of Mathematics and Computing Science, The University of the South Pacific, Suva, Fiji.

‖ This definition is certainly appropriate for patterns that are locally finite (which all patterns studied here are). There is a case for a broader concept of local indistinguishability when dealing with patterns that are no longer discrete.

0305-4470/97/093029+28$19.50

of the crystallographic pattern it derives from, hence, again by the points on a torus. The great beauty of this parametrization is that it can be readily used to count and classify patterns with special properties such as point or rescaling symmetries. Due to the connection with the torus, the determination of patterns with special symmetries is actually equivalent to the determination of (generalized) Wyckoff positions in the higher-dimensional lattice, and independent results on this [18, 12, 9] can be directly compared with our findings. It turns out that there are various little mistakes in [18, 12], but a computer program to generate the Wyckoff positions systematically (which will be available soon [9]) coincides with our figures.

In this article, we illustrate the torus parametrization for several relevant examples, bringing out the rich orbit structure of the LI-classes. A more complete and rigorous discussion of the general approach is then given in the appendix. In the body of the paper, which emerged from seminars given by the third author during his stay at Tübingen in spring 1994 and 1995, we focus on quasiperiodic tilings in one, two and three dimensions that show certain point symmetries (such as fivefold symmetry in the plane or icosahedral symmetry in three-space) as well as a local inflation/deflation symmetry related to the golden ratio, $\tau = (1+\sqrt{5})/2$. However, the method is very easy to apply to other cases of interest.

The article is organized as follows. In section 2 we set the scene for the torus parametrization, illustrating it for the well known Fibonacci chain. We calculate the number of tilings invariant under inversion and under n-fold inflation and discuss the corresponding orbit structure for small n explicitly. Section 3 deals with the analogous programme for two standard tilings in the plane, namely the Tübingen triangle tiling and Robinson's triangular decomposition of the rhombic Penrose tiling. In section 4 we consider icosahedrally symmetric tilings of three-space, namely Kramer's original tiling with two rhombohedra (which is of P-type and has only τ^3-inflation), as well as an F-type and an B-type icosahedral tiling. This is followed by some concluding remarks.

2. Fibonacci chains

The well known Fibonacci chain can be obtained from the square lattice $\mathbb{Z}^2$ by the standard strip projection method as shown in figure 1. After the choice of a one-dimensional (1D) subspace, E (in this case a line through the origin of irrational slope $1/\tau$) and a so-called internal space, $E_{\rm int}$ (in this case the orthogonal complement of E), one projects into E parallel to $E_{\rm int}$ all those lattice points whose projection into $E_{\rm int}$ parallel to E falls inside a certain window or acceptance domain, W (in this case the lattice points in the strip which circumscribes the square with side 1 and centre $(0, 0)$). This gives a discrete point set in E which is non-periodic, due to the irrational slope of E. The intervals between consecutive points are of two lengths in the ratio $\tau : 1$, which we label a (for the long one) and b (for the short one). This sequence of intervals is a *Fibonacci chain* which we label $\mathcal{F}_{aa}$. It is symmetric about the origin with two a's at the centre.

2.1. The LI-class

The other chains in the LI-class of $\mathcal{F}_{aa}$ are obtained by translating the 2D space $E + E_{\rm int}$ (which contains E and the strip) relative to the space $\mathbb{R}^2$ containing the lattice $\mathbb{Z}^2$, and carrying out the same construction with the new set of lattice points in the strip. In other words, we consider $E + E_{\rm int}$ (equipped with a reference point) as a sheet that can be moved on top of $\mathbb{R}^2$, relative to its origin. Chains obtained in this way are locally isomorphic to $\mathcal{F}_{aa}$. Two translations that differ by a lattice vector clearly give the same chain in E.

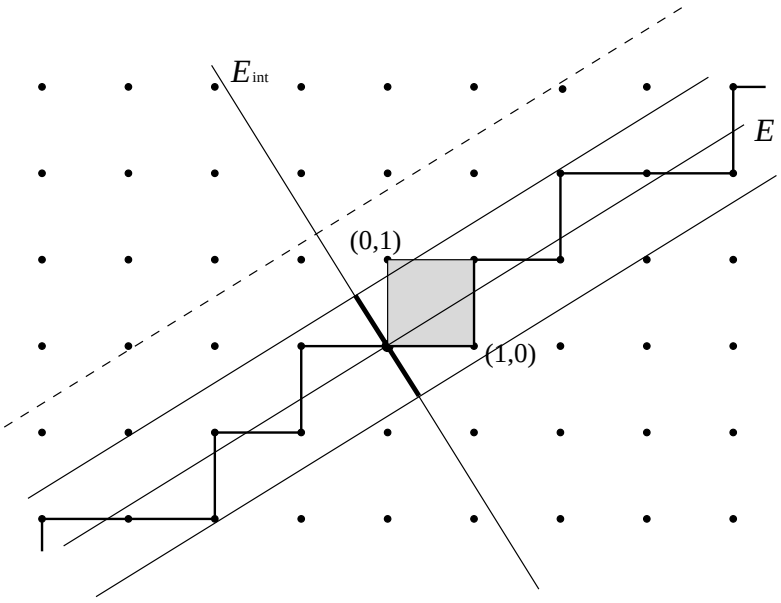

Figure 1. Projection scheme for the Fibonacci chain. The origin of the two-dimensional (2D) space $E + E_{\rm int}$ is depicted by the big black dot and may be moved relative to the lattice in the shaded torus region. The chain shown corresponds to the torus parameter $(0, 0)$. The window (width of the strip) is the projection of the Voronoi cell (not shown) around the origin into $E_{\rm int}$. The upmost line parallel to E (broken) is the upper boundary of the inflated strip.

Conversely, it can be shown (though we do not prove it here) that translations not differing by a lattice vector give distinct chains in E and that all chains in the LI-class of $\mathcal{F}_{aa}$ are obtained in this way [25].

We draw attention here to the so-called *singular* chains in the LI-class, which occur when a lattice point falls on the boundary of the strip causing an ambiguity as to whether to include the point in the chain. For these, more than one chain corresponds to the same parameter. In the case of 1D chains derived from the strip construction that are identified in this way, exactly two singular chains have the same parameter and they differ from each other in at most two points. Also, these singular chains form a lower-dimensional subset (in a sense to be made precise later) of the LI-class. All other chains are called *regular*.

More generally, singular patterns derived from the cut-and-project construction with polytopic windows differ from each other at most on a finite number of lower-dimensional subspaces and form finite classes. (So the ambiguities have the flavour of a surface effect.) We do not completely know how this is to be modified for more general shapes of windows (e.g. spherical or fractal). However, if the boundary of the window has Lebesgue measure 0 (and we will not consider any situation other than that), the identification of singular patterns is meaningful (in view of physical indistinguishability) and still almost all patterns of the LI-class are regular. In [21, 17] the convention is adopted of identifying singular patterns in the same class, enabling the correspondence between patterns and parameters to be regarded as one-to-one.

2.2. Torus parametrization

We now choose a reference point, $\boldsymbol{r}$, on E and associate with each point $\boldsymbol{t} \in \mathbb{R}^2$ the chain (or pair of singular chains) in E given by translating $\boldsymbol{r}$ to $\boldsymbol{t}$. Since adding a lattice vector in $\mathbb{Z}^2$ to $\boldsymbol{t}$ does not change the chain in E, by the preceding section this puts the points of the torus $\mathbb{T}^2 = \mathbb{R}^2/\mathbb{Z}^2$ in one-to-one correspondence with the regular chains and singular chain pairs in the LI-class of $\mathcal{F}_{aa}$. Adding a vector, $\boldsymbol{a} \in E$, to $\boldsymbol{t}$ clearly has the effect of translating the chain by $-\boldsymbol{a}$, but vectors $\boldsymbol{t}_1$, $\boldsymbol{t}_2$ whose difference is not in $E + \mathbb{Z}^2$ correspond to chains in different translation classes. Since τ is irrational, each translation class wraps around $\mathbb{T}^2$ infinitely many times in both directions without self-intersection (equivalent to the fact that the chains are not periodic).

We call the one-to-one correspondence with $\mathbb{T}^2$ the *torus parametrization* of the LI-class.

Note that the parametrization depends on the position of $\boldsymbol{r}$ on E and the position of the window W in $E_{\rm int}$: if $\boldsymbol{r}$ is moved to $\boldsymbol{r} + \boldsymbol{a}$ on E the parameters are shifted by $-\boldsymbol{a}$ on $\mathbb{T}^2$, if W is translated by $\boldsymbol{b}$ on $E_{\rm int}$ the parameters are shifted by $-\boldsymbol{b}$ on $\mathbb{T}^2$. This is analogous to parametrizing a Euclidean line by the real numbers: the LI-class of $\mathcal{F}_{aa}$, like the Euclidean line, is a uniform structure with no natural origin. *To standardize the parametrization of the Fibonacci chains we shall choose $\boldsymbol{r}$ to be the origin of E and the interval W to be symmetric about the origin of $E_{\rm int}$.* With this standardization $\mathcal{F}_{aa}$ itself has the parameter $\boldsymbol{t} = (0, 0)$.

2.3. Symmetry

The only kind of point symmetry possible for 1D chains is mirror symmetry, which we shall usually refer to as *inversion symmetry* in order to have the same terminology for all dimensions ('inversion' meaning the isometry $\boldsymbol{x} \mapsto -\boldsymbol{x}$). $\mathcal{F}_{aa}$ is inversion symmetric. Are there other inversion symmetric Fibonacci chains? Well, clearly the Fibonacci chains corresponding to points $\boldsymbol{t}$ and $-\boldsymbol{t}$ on the torus are mirror images, and since the torus parametrization is a one-to-one correspondence these are the only mirror image pairs of Fibonacci chains. (Thus, for our standard parametrization which has the reference point inversion symmetric in E and the window inversion symmetric in $E_{\rm int}$, inversion of Fibonacci chains in E derives from inversion in $\mathbb{R}^2$.) So inversion symmetric Fibonacci chains correspond to points $\boldsymbol{t}$ on the torus with $\boldsymbol{t} = -\boldsymbol{t}$, i.e. $2\boldsymbol{t} = \boldsymbol{0}$. There are four such points

$$(0, 0) \qquad (\tfrac{1}{2}, 0) \qquad (0, \tfrac{1}{2}) \qquad \text{and} \qquad (\tfrac{1}{2}, \tfrac{1}{2}) \tag{1}$$

that form the discrete subgroup of 'two-division points' of $\mathbb{T}^2$, isomorphic to $C_2 \times C_2$. The four corresponding symmetric chains, in the order of the parameters (1), are

$$\begin{aligned}
\mathcal{F}_{aa} &= \ldots baababaabaababa\underline{a}\underline{a}babaabaabababaab\ldots \\
\mathcal{F}_{a} &= \ldots ababaababaabaaba\underline{b}abaabaababaababa\ldots \\
\mathcal{F}_{b} &= \ldots aabaababaababaa\underline{b}aababaabababaabaa\ldots \\
\mathcal{F}_{ab} &= \ldots baabaababaaba\left\{\frac{ab}{ba}\right\}abaababaabaab\ldots.
\end{aligned} \tag{2}$$

Here $\mathcal{F}_{ab}$ is a pair of singular chains, the other three chains are regular.

2.4. Inflation

In addition to inversion symmetry, the Fibonacci chains show another feature typical of quasiperiodic patterns, namely an inflation/deflation symmetry. Let us explain this in the

projection picture. In figure 1 the original strip, S_1, representing a Fibonacci chain $\mathcal{F}$ ($\mathcal{F}_{aa}$ in fact) is enclosed in a strip S_τ, τ times as wide. The lattice points in S_τ give a refinement of the chain given by S_1. This refinement is itself a scaled version of a Fibonacci chain. To see this, consider the action of the matrix

$$M = \begin{pmatrix} 1 & 1 \\ 1 & 0 \end{pmatrix}. \tag{3}$$

It has an eigenvector† $\boldsymbol{e} = (\tau, 1)$ with eigenvalue τ in the direction of E, an eigenvector $\boldsymbol{e}_{\rm int} = (-1/\tau, 1)$ with eigenvalue $-1/\tau$ in the direction of $E_{\rm int}$, and, being integral and unimodular, acts as an automorphism on the lattice $\mathbb{Z}^2$. So MS_τ is a strip of the same width and direction as S_1 and represents a Fibonacci chain $\mathcal{F}'$. Since M maps the lattice points in S_τ one-to-one onto the lattice points of MS_τ, and since it preserves the projection direction and stretches distances in the E direction by a factor of τ, the chain given by the lattice points in S_τ is the chain $\mathcal{F}'$ shrunk by a factor of τ.

The two features of being locally isomorphic to $\mathcal{F}$ and scaling to a refinement of it (eventually up to a shift) make $\mathcal{F}'$ an *inflation* of $\mathcal{F}$.

How is the torus parameter of $\mathcal{F}'$ related to that of $\mathcal{F}$? Well, if $\mathcal{F}$ has the parameter $\boldsymbol{t}$ then the point on the centreline of S_τ that projects onto the origin of E is $\boldsymbol{t} + (\tau/2\sqrt{5})\boldsymbol{e}_{\rm int}$, so $\mathcal{F}'$ has the parameter

$$M\left(\boldsymbol{t} + \frac{\tau}{2\sqrt{5}}\boldsymbol{e}_{\rm int}\right) = M\boldsymbol{t} - \frac{\boldsymbol{e}_{\rm int}}{2\sqrt{5}}. \tag{4}$$

As $\mathcal{F}$ varies, the inflation given by enclosing the strip for $\mathcal{F}$ in a strip τ times as wide with the lower edges coinciding is represented on $\mathbb{T}^2$ by $\boldsymbol{t} \mapsto M\boldsymbol{t} + \boldsymbol{c}$, where $\boldsymbol{c} = -\boldsymbol{e}_{\rm int}/2\sqrt{5}$ is independent of $\boldsymbol{t}$.

Choosing a different fixed offset for the wide strip relative to the narrow one leads to a different inflation on the LI-class which is again represented on $\mathbb{T}^2$ by $\boldsymbol{t} \mapsto M\boldsymbol{t} + \boldsymbol{c}$, but with a different value of $\boldsymbol{c}$. The above refinement property of the inflation corresponds to the requirement that, in our picture, the wider strip must enclose the narrower one.

In terms of Fibonacci chains, the inflation illustrated, given by $\boldsymbol{c} = -\boldsymbol{e}_{\rm int}/2\sqrt{5}$, corresponds to the substitution rule

$$b \mapsto a \qquad a \mapsto ab. \tag{5}$$

The inflation given by $\boldsymbol{c} = \boldsymbol{e}_{\rm int}/2\sqrt{5}$, corresponds to the rule

$$b \mapsto a \qquad a \mapsto ba. \tag{6}$$

More generally, $\boldsymbol{c} = \beta\boldsymbol{e}_{\rm int}/2\sqrt{5}$ with $|\beta| \leqslant 1$ has the effect

$$b \mapsto a \qquad a \mapsto ab \text{ or } ba \tag{7}$$

the proportion of a's that change to ba being $(\beta + 1)/2$. Only countably many of these inflations are local, in the sense that whether a given a changes to ab or ba can be determined by looking at the part of $\mathcal{F}$ within a bounded distance of that a.

In particular, the symmetric inflation given by $\boldsymbol{c} = \boldsymbol{0}$, discussed in [17], in which half the a's change to ab and half to ba, is non-local. It can be described by the rule $a \mapsto x_{-j}x_j$ in (7), where $x_{-j}x_{-j+1}\ldots x_{-1}ax_1\ldots x_{j-1}x_j$ is the shortest segment of $\mathcal{F}$ centred on the a to be inflated for which $x_{-j} \neq x_j$. It is non-local because a Fibonacci chain has arbitrarily long symmetric neighbourhoods centred on a's. In particular, for the central a of $\mathcal{F}_a$ the symmetry never breaks and the rule is undecidable, resulting in inflation to a singular chain with two possibilities.

† For later convenience, we do not use unit vectors here.

Inflations derived from other values of $\boldsymbol{c}$, with a non-zero part parallel to $\boldsymbol{e}$, consist of one of these followed by a translation. Note that the decomposition into substitution and translation is not unique: for example, inflation (6) is identical to (5) translated by the length of a. This non-uniqueness reflects the fact that $\boldsymbol{c}$ can be written in many ways as $\alpha\boldsymbol{e} + \beta\boldsymbol{e}_{\mathrm{int}}/2\sqrt{5} \pmod{\mathbb{Z}^2}$, where $|\beta| \leqslant 1$ to guarantee the refinement property, but $\alpha \in \mathbb{R}$ arbitrary. However, distinct points $\boldsymbol{c}$ of $\mathbb{T}^2$ give distinct inflations.

The above discussion makes the following definition natural.

Definition. An *inflation* on the LI-class of Fibonacci chains is a mapping $\mathbb{T}^2 \to \mathbb{T}^2$ of the form

$$\boldsymbol{t} \mapsto A\boldsymbol{t} + \boldsymbol{c} \tag{8}$$

where $\boldsymbol{c} \in \mathbb{T}^2$ and A is a non-singular 2×2 integer matrix with eigenvectors $\boldsymbol{e}$ and $\boldsymbol{e}_{\mathrm{int}}$. A *family of inflations* is a set of inflations that share the same matrix, A, but have $\boldsymbol{c}$ running through all points of $\mathbb{T}^2$.

This definition makes plain that each family of inflations, such as the LI-class itself, is parametrized by $\mathbb{T}^2$. As mentioned above, the inflation (given by a certain $\boldsymbol{c}$) may be looked at in (countably many) different ways in the space E as a transformation on the chains.

In our present example, the situation is as follows. Given $\boldsymbol{c} \in \mathbb{T}^2$, there are countably many values $\boldsymbol{c}' \in \mathbb{R}^2$ with $\boldsymbol{c}' = \alpha\boldsymbol{e} + \beta\boldsymbol{e}_{\mathrm{int}}/2\sqrt{5} \equiv \boldsymbol{c} \pmod{\mathbb{Z}^2}$, $|\beta| \leqslant 1$. Every choice of $\boldsymbol{c}'$ represents a different view of the same inflation, where β tells us the proportion of a's that change to ab, and $-\alpha\tau/\sqrt{\tau+2}$ gives the distance of the inflation fixed point to the origin. (Although there is no natural choice, we shall usually take the representative with minimal $|\alpha|$.)

Changing $\boldsymbol{c}$ by a scalar multiple of $\boldsymbol{e}$ merely changes the translation component of the inflation, but other changes to $\boldsymbol{c}$ change the inflation more fundamentally. Due to the conditions mentioned above, A must in fact take the form

$$A = r\mathbb{1} + sM \qquad r, s \in \mathbb{Z} \tag{9}$$

where M is the matrix of τ-inflation as in equation (3). A represents an invertible inflation/deflation symmetry if and only if $A = \pm M^m$ with $m \in \mathbb{Z}$. We call the eigenvalue of A in E the inflation *multiplier*.

The inflation, given by its representation on $\mathbb{T}^2$, generates an infinite Abelian group isomorphic with C_∞ which acts on the LI-class. This gives rise to some kind of generalized symmetry [1], but not to a point symmetry because it cannot be represented as an isometry. In the sequel, we shall call chains (or patterns) I^n-symmetric if they are invariant under n-fold inflation. Simultaneously, we shall use the same symbol to denote the group generated by I^n, where I stands for the special inflation under consideration (i.e. M in this case). Note that, as groups, they are all isomorphic with the infinite cyclic group C_∞.

2.5. Applications of the torus parametrization

The usefulness of the torus parametrization stems from the simple behaviour of what might be called the 'affine torus operators' (8).

Fundamental fact. An operator of the form of (8), where A is any non-singular 2×2 integer matrix with $|\det A| = d$, is a d-fold cover of $\mathbb{T}^2$ by itself, in the sense that, for each $\boldsymbol{w} \in \mathbb{T}^2$, there are exactly d distinct solutions $\boldsymbol{t} \in \mathbb{T}^2$ of

$$A\boldsymbol{t} + \boldsymbol{c} = \boldsymbol{w}. \tag{10}$$

We give a proof of this in the appendix. Note that the number of solutions is not only independent of $\boldsymbol{w}$ but also independent of the constant term, $\boldsymbol{c}$, of the operator.

Here are some immediate applications of the fundamental fact. When interpreting them for Fibonacci chains we need to bear in mind that the two singular chains are attached to one parameter and must be treated as a single entity. As above, the following equations are to be understood mod $\mathbb{T}^2$.

How many Fibonacci chains are inversion symmetric? As we have seen, these correspond to points $\boldsymbol{t} \in \mathbb{T}^2$ with $2\boldsymbol{t} = \boldsymbol{0}$. Taking $A = 2\mathbb{1}$ and $\boldsymbol{c} = \boldsymbol{0}$ tells us that there are $|\det(2\mathbb{1})| = 4$ of these.

Is inflation of Fibonacci chains invertible? Since $|\det M| = 1$ there is exactly one solution of $M\boldsymbol{t} + \boldsymbol{c} = \boldsymbol{w}$ for each $\boldsymbol{w}$, so every inflation in the family (for any $\boldsymbol{c}$ whatever) is a one-to-one correspondence from $\mathbb{T}^2$ to itself and each Fibonacci chain comes from a unique precursor under the inflation.

How many Fibonacci chains are inflation-invariant? We need to count the solutions of $M\boldsymbol{t} + \boldsymbol{c} = \boldsymbol{t}$, which can be rewritten as $(M - \mathbb{1})\boldsymbol{t} + \boldsymbol{c} = \boldsymbol{0}$. Since $|\det(M - \mathbb{1})| = 1$ there is precisely one inflation-invariant chain. For the non-local symmetric inflation $\boldsymbol{c} = \boldsymbol{0}$ this is $\mathcal{F}_{aa}$; for the local inflation $\boldsymbol{c} = (\frac{1}{2}, 0) = (\boldsymbol{e} - \boldsymbol{e}_{\mathrm{int}})/2\sqrt{5}$ it is the singular chain $\mathcal{F}_{ab}$.

As well as each inflation, $\boldsymbol{c}$, having a unique fixed point, namely $\boldsymbol{a} = -M\boldsymbol{c}$, for each point $\boldsymbol{a}$ of $\mathbb{T}^2$, there is a unique inflation that leaves it invariant, namely that given by $\boldsymbol{c} = \boldsymbol{a} - M\boldsymbol{a}$.

How many Fibonacci chains have inflation orbits of length 2? Or, in other words, how many Fibonacci chains are I^2-symmetric? The relevant equation is $(M^2 - \mathbb{1})\boldsymbol{t} + \boldsymbol{c} = \boldsymbol{0}$. Since $|\det(M^2 - \mathbb{1})| = 1$ there is only one solution. But this must represent the inflation-invariant chain, so there are no chains with an inflation orbit of length 2.

How many Fibonacci chains are I^3-symmetric? Since $|\det(M^3 - \mathbb{1})| = 4$ there are four chains left invariant by triple inflation. There is only one inflation-invariant chain, so the remaining three form a single orbit of length 3.

We can say more about what these last four chains are. The symmetric inflation with $\boldsymbol{c} = \boldsymbol{0}$ acting on a symmetric chain gives another symmetric chain. (This is clear either directly from the strip construction or from the observation that M commutes with $-\mathbb{1}$, the inversion.) So the set of four inversion symmetric chains is stabilized by this inflation. In view of the foregoing, one must be inflation-invariant and the others a three-cycle under inflation. In fact, $\mathcal{F}_{aa}$ is invariant under symmetric inflation and $(\mathcal{F}_b, \mathcal{F}_a, \mathcal{F}_{ab})$ is a three-cycle.

Are there other inflations in the family that commute with inversion? If so then $M(-\boldsymbol{t}) + \boldsymbol{c} = -(M\boldsymbol{t} + \boldsymbol{c})$ for all $\boldsymbol{t}$, giving $\boldsymbol{c} = -\boldsymbol{c}$, so $\boldsymbol{c}$ must be one of the two-division points of $\mathbb{T}^2$. These come from the points of $\mathbb{R}^2$ that are centres of inversion symmetry of the lattice $\mathbb{Z}^2$. We have already seen that $\boldsymbol{c} = (\frac{1}{2}, 0)$ gives a local inflation that fixes $\mathcal{F}_{ab}$. The statistics for all four of these inflations are given in table 1. There, we also list the fixed points $(\boldsymbol{a})$ of the inflations which coincide with the torus parameters of the corresponding inflation invariant Fibonacci chains. Furthermore, we give more special information on which fraction of a's inflate to ba for the representative specified by the distance of the inflation fixed point to the origin in E.

These are the only inflations in the family that stabilize the set of symmetric chains. Only the second of them, $\boldsymbol{c} = (\frac{1}{2}, 0)$, is local. It is interesting to note that the cubes of these inflations are all the same and all equal to the translationless inflation given by the symmetric local rule $b \mapsto aba$, $a \mapsto ababa$, which fixes all four symmetric chains.

We see here a connection between symmetric patterns and short inflation orbits that will also feature in higher-dimensional patterns. What has happened is this. There is a small

Table 1. Inversion symmetric inflations of the Fibonacci LI-class.

$\boldsymbol{c}$	Infl. fixed point ($\boldsymbol{a}$)	Proportion of a's that inflate to ba	Shift in E	Action on the symmetric chains	Local?
$(0,0)$	$(0,0)$	$\frac{1}{2}$	0	$(\mathcal{F}_{aa})(\mathcal{F}_b,\mathcal{F}_a,\mathcal{F}_{ab})$	No
$(\frac{1}{2},0)$	$(\frac{1}{2},\frac{1}{2})$	0	$(\tau^2/2)e$	$(\mathcal{F}_{ab})(\mathcal{F}_a,\mathcal{F}_b,\mathcal{F}_{aa})$	Yes
$(0,\frac{1}{2})$	$(\frac{1}{2},0)$	$1/2\tau$	$(\tau^4/2)e$	$(\mathcal{F}_a)(\mathcal{F}_b,\mathcal{F}_{ab},\mathcal{F}_{aa})$	No
$(\frac{1}{2},\frac{1}{2})$	$(0,\frac{1}{2})$	$\tau/2$	$(\tau^3/2)e$	$(\mathcal{F}_b)(\mathcal{F}_a,\mathcal{F}_{aa},\mathcal{F}_{ab})$	No

number of symmetric chains. This set of chains is stabilized by the symmetric inflation (since it commutes with inversion) and hence decomposes into short inflation orbits. The set of symmetric chains is a group on the torus and hence stabilized by the corresponding translations. Consequently it is stabilized not only by the symmetric inflation but also by the inflation obtained by combining it with each of these translations. Fortuitously, one of these inflations is local.

2.6. Counting inflation orbits

The answers to the last three questions above immediately generalize: the number of Fibonacci chains with I^n-symmetry is $|\det(M^n - \mathbb{1})|$. Furthermore, there is a uniform way of computing these determinants. Since the eigenvalues of M are τ and its algebraic conjugate $\tau' = -1/\tau$, and since the determinant of a matrix is the product of its eigenvalues, we have

$$\det(M^n - \mathbb{1}) = (\tau^n - 1)((\tau')^n - 1) \tag{11}$$

$$= N_2[\tau^n - 1] \tag{12}$$

where, for $\alpha = r + s\tau \in \mathbb{Q}(\tau)$, $N_2[\alpha]$ is the *norm* of α defined as

$$N_2[\alpha] = \alpha\alpha' = (r + s\tau)(r + s\tau') = r^2 + rs - s^2. \tag{13}$$

Here, $\mathbb{Q}(\tau) = \{a + b\tau | a, b \in \mathbb{Q}\} = \mathbb{Q}(\sqrt{5})$ is the quadratic field of degree 2 over the rationals generated by τ. Note that $N_2[\alpha]$ is an integer if r, s in (13) are integers. For details on this and how to formulate the cut-and-project scheme systematically in number theoretic terms† we refer the reader to [22].

The number, a_n, of Fibonacci chains with I^n-symmetry is thus given by

$$a_n = |N_2[\tau^n - 1]| = -N_2[\tau^n - 1] = \tau^n + (\tau')^n - 1 - (-1)^n \tag{14}$$

which differs from τ^n by less than 2. Being the roots of the equation $x^2 - x - 1 = 0$, τ and τ' both satisfy $x^n = x^{n-1} + x^{n-2}$, and hence a_n satisfies the recurrence

$$a_n = a_{n-1} + a_{n-2} + 1 - (-1)^n. \tag{15}$$

This allows us to compute it very quickly starting from the values $a_1 = a_2 = 1$ which we already have. The values up to $n = 15$ are given in table 2. (In terms of the Fibonacci numbers, f_n, we have $a_n = f_{n+1} + f_{n-1} - 1 - (-1)^n$, since this sequence satisfies the same recurrence and has the same starting values.)

As already glimpsed in the cases $n = 2$ and $n = 3$, the chains with inflation orbits of length n are those invariant under n-fold inflation but not under m-fold inflation for any

† Although we shall use this alternative approach quite frequently, we cannot give a full account of it in this article.

Table 2. Inflation orbit counts for 1D cut-and-project patterns with τ-inflation.

n	1	2	3	4	5	6	7	8	9	10	11	12	13	14	15
a_n	1	1	4	5	11	16	29	45	76	121	199	320	521	841	1364
b_n	1	0	3	4	10	12	28	40	72	110	198	300	520	812	1350
c_n	1	0	1	1	2	2	4	5	8	11	18	25	40	58	90

proper factor, m, of n. Let b_n be the number of chains invariant under n-fold inflation but not under m-fold inflation for any $m < n$. Then

$$b_n = a_n - \sum_{\substack{m<n \\ m|n}} b_m \tag{16}$$

allowing us to calculate the b_n's from the a_n's recursively. (Here $m|n$ means m divides n.) Finally, since b_n counts chains in inflation orbits of length n it must be divisible by n and

$$c_n = \frac{b_n}{n} \tag{17}$$

is the number of orbits. Table 2 also lists b_n and c_n, the fact that the latter are integers, despite being obtained by being divided by n, provides a check on our arithmetic.

The action of inflation on $\mathbb{T}^2$ is a dynamical system and the explicit expression (14) enables us to write down its Artin–Mazur ζ-function (compare with [20, ch 5] for the concept and some general results)

$$Z_1(x) = \frac{1-x^2}{1-x-x^2}. \tag{18}$$

This gives the a_n's through the expansion

$$\log Z_1(x) = \sum_{n=1}^{\infty} \frac{a_n}{n} x^n = x + \tfrac{1}{2}x^2 + \tfrac{4}{3}x^3 + \tfrac{5}{4}x^4 + \tfrac{11}{5}x^5 + \cdots \tag{19}$$

and the c_n's through the Euler product decomposition

$$\frac{1}{Z_1(x)} = \prod_{n=1}^{\infty}(1-x^n)^{c_n} = (1-x)^1(1-x^2)^0(1-x^3)^1(1-x^4)^1(1-x^5)^2\ldots. \tag{20}$$

It has the functional equation $Z_1(x) = Z_1(-1/x)$ and conforms to the 'Riemann hypothesis' that its zeros α satisfy $N_2[\alpha] = 1$. The pole of $\log Z_1(x)$ closest to zero is $x = 1/\tau$, confirming the growth rate $a_n \sim \tau^n$ as $n \to \infty$.

Let us briefly remark that we can also obtain a power series generating function for the a_n's through the logarithmic derivative of $Z_1(x)$ as follows:

$$F_1(x) = \frac{xZ'_1(x)}{Z_1(x)} = \sum_{n=1}^{\infty} a_n x^n. \tag{21}$$

Then, one may also obtain a generating function for the b_n's in terms of a Lambert series, compare with [10].

2.7. Interaction between inflation and point symmetry

We now investigate the orbit structure of the Fibonacci LI-class under the generalized symmetry group $C_2 \times I^1$ generated by inversion and inflation (compare also with [1] for this concept).

One might expect c_n to be even, since Fibonacci chains occur in mirror image pairs, so, for the inflations that commute with inversion, each orbit has a mirror image orbit of the same length. The oddness of c_1 and c_3 is accounted for by the fact that the orbits they count consist of symmetric chains. But we know there are no other symmetric chains. The oddness of other c_n's must be accounted for by the fact that an inflation orbit can be 'symmetric' even though the chains in it are not. This occurs when n is even and the mirror image of a chain in the orbit is also a multiple inflation of the same chain, that is (in the case of the inflation $\boldsymbol{c} = \boldsymbol{0}$)

$$M^m \boldsymbol{t} = -\boldsymbol{t} \tag{22}$$

for some m. As inversion commutes with inflation, this can only happen for $m = n/2$, where n is the length of the inflation orbit of $\boldsymbol{t}$. The full symmetry of a chain in such an orbit is then $-I^{n/2}$ rather than I^n, where $-I^k$ stands for the group generated by the inversion-inflation $-M^k$ and $I^n = (-I^{n/2})^2$.

To count the symmetric inflation orbits let $\tilde{a}_n$ be the number of solutions to (22) with $m = n/2$ (and $\tilde{a}_n = 0$ when n is odd). Using the fundamental fact we have, for even n,

$$\tilde{a}_n = |\det(M^{n/2} + \mathbb{1})| \tag{23}$$

$$= N_2[\tau^{n/2} + 1] \tag{24}$$

$$= \tau^{n/2} + (\tau')^{n/2} + 1 + (-1)^{n/2} \tag{25}$$

which satisfies the recurrence

$$\tilde{a}_{2k} = \tilde{a}_{2(k-1)} + \tilde{a}_{2(k-2)} - 1 + (-1)^k \tag{26}$$

starting with $\tilde{a}_2 = 1$, $\tilde{a}_4 = 5$. If now $\tilde{b}_n$ is the number of points $\boldsymbol{t} \in \mathbb{T}^2$ that satisfy (22) with $m = n/2$ and have exact order n under inflation then $\tilde{b}_n$ can be computed much as b_n was (with a slight extra complication† in allowing for the symmetric chains) and the number of symmetric orbits of length n is given by

$$\tilde{c}_n = \frac{\tilde{b}_n}{n}. \tag{27}$$

Some values of $\tilde{a}_n$, $\tilde{b}_n$ and $\tilde{c}_n$ are listed in table 3, and we see that $c_n - \tilde{c}_n$, being the number of orbits of chains whose full symmetry is I^n, is even in all cases listed. These numbers, like those in table 2, are the same for every inflation in the family.

Tables 2 and 3 give complete information on the various orbit counts for the Fibonacci chain. We note that these figures do not depend on $\boldsymbol{c}$, so are the same for every inflation in the family (although, of course, the orbits themselves are different for different inflations). What is more; these orbit counts are functions of the inflation multiplier, τ, alone and thus also apply to all other LI-classes of chains with τ-inflation and embedding dimension two.

So far we have worked with single chains, but the results also extend to translation classes of chains, with no changes to the counts. Details of this are given in the appendix.

† The explicit rule is as follows. In the first step, one subtracts either 4 from $\tilde{a}_n$ (if n is divisible by 6) or 1 (otherwise). In the second step, one subtracts any $\tilde{b}_m$ from $\tilde{a}_n$ where $m < n$ and $n = km$ with k odd.

Table 3. Symmetric inflation orbit counts for 1D cut-and-project patterns with inversion symmetric τ-inflation.

n	2	4	6	8	10	12	14	16	18	20	22	24	26	28	30
$\tilde{a}_n$	1	5	4	9	11	20	29	49	76	125	199	324	521	845	1364
$\tilde{b}_n$	0	4	0	8	10	12	28	48	72	120	198	312	520	840	1350
$\tilde{c}_n$	0	1	0	1	1	1	2	3	4	6	9	13	20	30	45

3. Planar tilings with τ-inflation and tenfold symmetry

The torus parametrization is more powerful for the description of patterns and tilings in two and higher dimensions. The main reason is the possibility of non-trivial symmetries. In the previous section, we described the general set-up, with focus on the projection picture. In particular, we have used a projection-based approach to inflation, very much in the spirit of [21, 17]. Although this is very systematic, there is a consequence: an inflation constructed that way is usually not local, and one has to decide upon locality afterwards. This is in general not so easy to do, in particular when the pattern lives in higher dimension.

There exists, however, also a slightly different point of view. Instead of generalizing the projection-based concept of inflation (as in [17]), one can consider *local* inflation rules as defined in [5], i.e. one actually starts from examples where the LI-class of a pattern is defined through the fixed point of a local inflation rule. Since this is widely used in literature, we will now adopt this point of view. Clearly, before we can apply the torus parametrization, we have to know that the LI-class under consideration can be obtained equally as well by the projection scheme. But that can be decided upon rather easily [5], and it will be fulfilled in all examples below. So, the torus parametrization may be employed again to investigate the structure of the LI-class. Let us first see how this works in 2D, where we first present a suitable set-up for the projection used.

3.1. Projection method

To use the cut-and-project construction to obtain a non-periodic 2D pattern, $\mathcal{P}$, from a four-dimensional (4D) lattice, Λ, we require two 2D subspaces $E, E_{\rm int} \subset \mathbb{R}^4$, such that the intersection of any two of Λ, E, $E_{\rm int}$ is $\{\mathbf{0}\}$, and a window $W \subset E_{\rm int}$. Then $\mathcal{P}$ consists of the projection on E parallel to $E_{\rm int}$ of all points of Λ whose projections on $E_{\rm int}$ parallel to E fall inside W. The other patterns in the LI-class of $\mathcal{P}$ are obtained by translating $E + W$ relative to Λ before carrying out this operation. The patterns are labelled by the point in $\mathbb{R}^4$ to which the origin of E is translated. With the exception of the singular patterns (those for which a point of Λ lies on the boundary of $E + W + \boldsymbol{r}$) two patterns in the LI-class are the same if and only if their labels are identical mod Λ. So the LI-class of $\mathcal{P}$ is parametrized by $\mathbb{T}^4 = \mathbb{R}^4/\Lambda$, a 4D torus, (with the proviso, as before, that nearly identical singular patterns share the same parameter).

An *inflation* on the LI-class of $\mathcal{P}$ is a mapping $\mathbb{T}^4 \to \mathbb{T}^4$ of the form

$$\boldsymbol{t} \mapsto A\boldsymbol{t} + \boldsymbol{c} \tag{28}$$

where $\boldsymbol{c} \in \mathbb{T}^4$ and A is a linear operator on $\mathbb{R}^4$ such that E and $E_{\rm int}$ are eigenspaces of A and $A\Lambda \subseteq \Lambda$. The eigenvalue of A on E is the *multiplier* of the inflation.

Again we use the fundamental fact that, just as in the 1D case, if B is any linear operator

Table 4. Inflation orbit counts for 2D cut-and-project patterns with τ-inflation.

n	1	2	3	4	5	6	7	8	9	10
a_n^2	1	1	16	25	121	256	841	2025	5776	14 641
$b_n^{(2)}$	1	0	15	24	120	240	840	2000	5760	14 520
$c_n^{(2)}$	1	0	5	6	24	40	120	250	640	1 452

on $\mathbb{R}^4$ with $B\Lambda \subseteq \Lambda$ then

$$\boldsymbol{t} \mapsto B\boldsymbol{t} + \boldsymbol{c} \tag{29}$$

gives a well-defined mapping $\mathbb{T}^4 \to \mathbb{T}^4$ that is a d-fold cover of $\mathbb{T}^4$ by itself, where $d = |\det B|$.

3.2. The multiplier τ case

We now suppose that A has eigenvalues τ and τ' on the eigenspaces E and E_{int}. An immediate application of the fundamental fact is that since $\det A = \tau^2(\tau')^2 = 1$ inflation is a one-to-one map from $\mathbb{T}^4$ to itself and hence is invertible.

Let $a_n^{(2)}$ be the number of patterns of the LI-class invariant under n-fold inflation. Then the above fact tells us that

$$\begin{aligned} a_n^{(2)} &= |\det(A^n - \mathbb{1})| = |\text{Product of the eigenvalues of } (A^n - \mathbb{1})| \\ &= (\tau^n - 1)^2((\tau')^n - 1)^2 = N_2[\tau^n - 1]^2 = a_n^2 \end{aligned} \tag{30}$$

so the numbers $a_n^{(2)}$ are the squares of the numbers obtained in table 2 for the 1D case. From these the number $b_n^{(2)}$ of patterns invariant under n-fold inflation but not under m-fold inflation for any $m < n$ and the number $c_n^{(2)}$ of inflation orbits of length n can be calculated as before. The first few of these numbers are given in table 4. Since $a_n^{(2)} \sim \tau^{2n}$ as $n \to \infty$, $c_n^{(2)} \sim \tau^{2n}/n$.

The ζ-function of this inflation operator is

$$Z_2(x) = \frac{(1 - x - x^2)^2(1 + x - x^2)^2}{(1 - 3x + x^2)(1 - x)^2(1 + x)^4} \tag{31}$$

with functional equation $Z_2(x) = Z_2(1/x)$ and Riemann hypothesis $N_2[\alpha] = -1$ for all zeros α. The pole of $\log Z_2(x)$ closest to zero is $x = 1/\tau^2$, confirming that the a_n grow like τ^{2n}.

3.3. The cyclotomic field $\mathbb{Q}(e^{2\pi i/5})$

To count the patterns with a given point symmetry we need to lift the symmetry to an operator, A, acting on the lattice, Λ, used for the cut-and-project construction (for example, inversion lifts to $-\mathbb{1}$). Then, with a special matrix representation (e.g. as given in [3]), one can calculate the various counts as determinants of matrices.

For the familiar planar patterns with decagonal symmetry, however, there is a good way of simplifying this by exhibiting the determinant as the norm of a number in the degree 4 cyclotomic field

$$\mathbb{Q}(\xi) = \{q_1 + q_2\xi + q_3\xi^2 + q_4\xi^3 | \xi = \mathrm{e}^{2\pi \mathrm{i}/5},\ q_1, q_2, q_3, q_4 \in \mathbb{Q}\}. \tag{32}$$

This field has $\mathbb{Q}(\tau)$ as a real subfield, and indeed

$$\mathbb{Q}(\tau) = \mathbb{Q}(\xi) \cap \mathbb{R}. \tag{33}$$

There is an automorphism σ of $\mathbb{Q}(\xi)$, fixing $\mathbb{Q}$, defined by $\sigma(\xi) = \xi^2$, which generates a cyclic group of automorphisms of the order of 4 (σ^2 is complex conjugation, σ^4 is the identity) called the *Galois group* of $\mathbb{Q}(\xi)$ over $\mathbb{Q}$. The effect of σ on $\mathbb{Q}(\tau)$ is that $\sigma(\tau) = \tau' = -1/\tau$, where $'$ is the algebraic conjugation in $\mathbb{Q}(\tau)$ used above. The absolute algebraic norm of a number $\alpha \in \mathbb{Q}(\xi)$ is now defined by

$$N_4[\alpha] = \alpha\sigma(\alpha)\sigma^2(\alpha)\sigma^3(\alpha) = \alpha\overline{\alpha}(\alpha\overline{\alpha})' = N_2[|\alpha|^2]. \tag{34}$$

The integers of $\mathbb{Q}(\xi)$ are $\mathbb{Z}[\xi] = \{u_1 + u_2\xi + u_3\xi^2 + u_4\xi^3 | u_1, u_2, u_3, u_4 \in \mathbb{Z}\}$ and norms of integers are rational integers, i.e. numbers in $\mathbb{Z}$.

Now if we represent $\mathbb{R}^4$ as $\mathbb{C}^2$ and put

$$\Lambda_4 = \{(\alpha, \sigma(\alpha)) | \alpha \in \mathbb{Z}[\xi]\} \tag{35}$$

then Λ_4 is the root lattice A_4 (see also [22]) and its orientation is such that, with the two copies of $\mathbb{C}$ as E and E_{int}, cut-and-project (with appropriate windows) gives the well known decagonal planar patterns [5]. Choosing the regular decagon whose vertices are the 10th roots of 1 as the window in E_{int} gives a point set in E that is in the MLD-class of the Penrose tiling, illustrated in figure 2 in the form of Robinson's triangular decomposition which is another representative of that class. Choosing as the window the regular decagon with centre 0 and one vertex $(1 + \xi)/\tau$ gives a point set in the MLD-class of the Tübingen triangle tiling (also illustrated in figure 2), namely its set of vertex points.

Given a $\lambda \in \mathbb{Z}[\xi]$ we obtain a linear operator A_λ on $\mathbb{C}^2$ which coincides with multiplication by λ on the first factor and multiplication by $\sigma(\lambda)$ on the second. Then $A_\lambda\Lambda_4 \subseteq \Lambda_4$ and hence A_λ acts on $\mathbb{T}^4$. Also

$$\det A_\lambda = |\lambda|^2|\sigma(\lambda)|^2 = N_4[\lambda]. \tag{36}$$

For example, A_1 is the identity operator $\mathbb{1}$ and A_τ is the inflation operator.

3.4. Rotation symmetry

Let us describe in some detail the examples just mentioned, namely the Tübingen triangle tiling (abbreviated TTT) and Robinson's decomposition of the rhombic Penrose tiling (RD), in order to use them as illustrations when looking at symmetric patterns. They

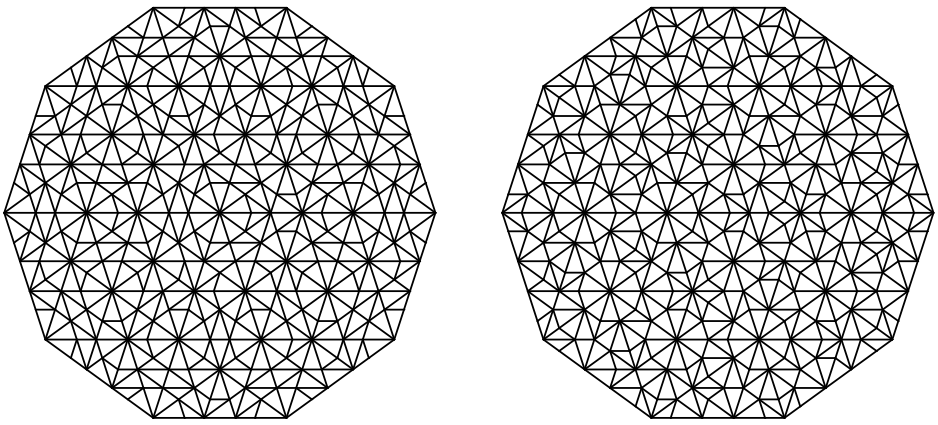

Figure 2. Decagonal versions of the Tübingen triangle tiling (TTT, left) and Robinson's decomposition of the rhombic Penrose tiling (RD, right). Both are singular, exactly symmetric under reflection in the x-axis, and exist in 10 rotated variants each.

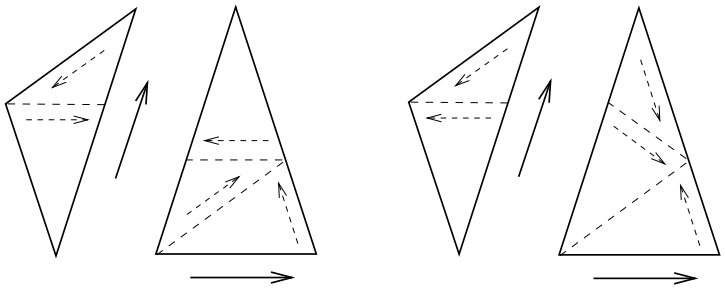

Figure 3. Local inflation rules for TTT (left) and RD (right).

are constructed through iterated inflation with the rules shown in figure 3. Although the differences between the two local inflation rules look small, they define two different LI-classes that do not even belong to equivalent tiling classes with respect to mutual local derivability [5]. These inflations both correspond to choosing $\boldsymbol{c} = \mathbf{0}$ in (28).

Due to fivefold symmetry, it is not possible to realize these tilings as sections of periodic structures of dimensions less than four (see [2, appendix A]). Consequently, the torus $\mathbb{T}^4$ is a generically one-to-one parametrization of these LI-classes.

We now count patterns with particular point symmetries and note their inflation orbits. The full point symmetry group of these LI-classes is D_{10}, generated by a tenfold rotation (called R) and reflection in the x-axis (S).

3.4.1. C_{10} symmetry. The number of patterns invariant under rotation of order 10 is

$$|N_4[-\xi^3 - 1]| = |N_2[\tau + 1]| = 1. \tag{37}$$

(Note that $\mathrm{e}^{2\pi \mathrm{i}/10} = -\xi^3$.) So only the point $\boldsymbol{t} = \mathbf{0}$ in $\mathbb{T}^4$ gives a pattern with C_{10} symmetry. Due to our choice of an inflation with $\boldsymbol{c} = \mathbf{0}$ it is clear that this is also reflection symmetric and inflation invariant. Thus, the full symmetry of the pattern is $D_{10} \times I^1$. In the RD tiling case this corresponds to the set of 10 singular tilings collectively known as the 'cartwheel'. In the Tübingen tiling case it is also a set of 10 singular tilings. A representative of each is shown in figure 2.

3.4.2. C_5 symmetry. The number of patterns invariant under rotation of order 5 is

$$|N_4[\xi - 1]| = |N_2[3 - \tau]| = 5. \tag{38}$$

One of these is the one with D_{10} symmetry. Since inflation commutes with R and S, the other four are permuted by inflation and hence form a single inflation orbit of length 4. (Table 4 tells us that there is one singleton orbit—already accounted for—and no doubleton.) Consequently, the space-inverted versions of these patterns have to lie in the same inflation orbit. Since no pattern is inversion symmetric itself, all patterns must be $(-I^2)$-symmetric. By means of the explicit matrix representation one also finds invariance under the reflection $-S$. Consequently, their full symmetry is $D_5 \times (-I^2)$. The corresponding TTT patterns are singular, see figure 4, while the corresponding RD tilings are regular, see figure 5, and consist of the 'sun', the 'star' and their S reflections.

3.4.3. C_2 symmetry. This is 2D inversion symmetry so the number of patterns with this symmetry is

$$N_4[2] = N_2[4] = 16 \tag{39}$$

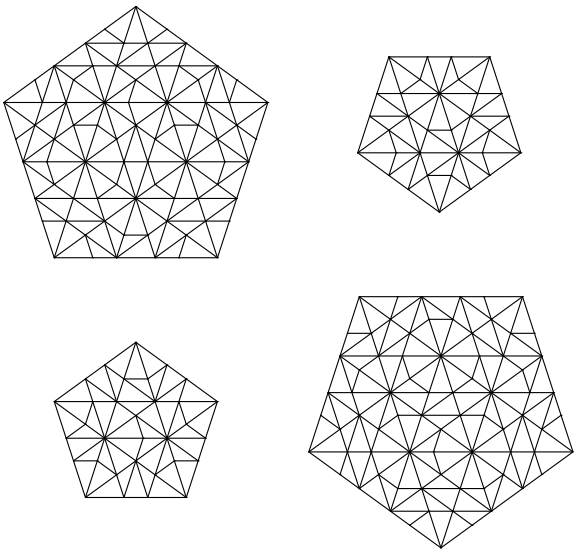

Figure 4. The four members of LI(TTT) with fivefold symmetry (singular). They form a four-cycle under inflation (shown in a clockwise arrangement). Each exists in five rotated versions and their mirror images.

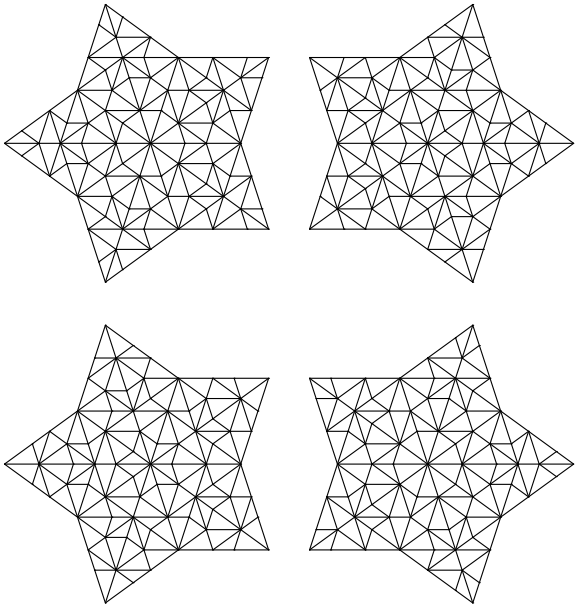

Figure 5. The four members of LI(RD) with fivefold symmetry (regular). They also form a four-cycle (clockwise) under inflation.

and the corresponding points of $\mathbb{T}^2$ are the two-division points. One of these gives the D_{10} pattern, while the remaining 15 consist† of the five inflation orbits of length 3. These five orbits are related by the rotations of the order of 5, since clearly none is invariant under fivefold rotation itself. Since 15 is odd and inversion commutes with the reflection S, at least one of these patterns is invariant under S so has D_2 symmetry. Then all three patterns in its inflation orbit have this same D_2 symmetry and those in the other inflation orbits have conjugate D_2 symmetries, i.e. a different reflection axis. Thus, all patterns with C_2

† It is a general fact of central τ-inflation in n dimensions that the patterns with I^3 symmetry are precisely the inversion-symmetric ones: since $\tau^3 - 1 = 2\tau$ and since τ is a unit, the equations $I^3\boldsymbol{t} = \boldsymbol{t}$ and $-\boldsymbol{t} = \boldsymbol{t}$ have the same set of solutions on $\mathbb{T}^{2n}$.

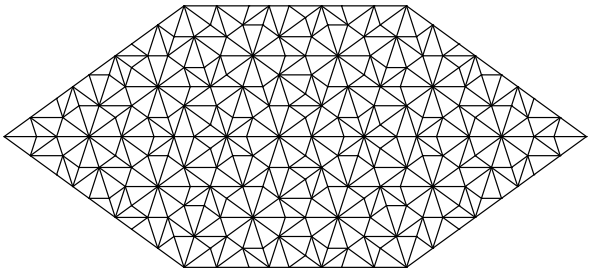

Figure 6. A Robinson tiling with $C_2 \times C_2$ symmetry. Reflection in the x-axis is exact, the one in the y-axis leaves a single worm of mismatches along the y-axis.

symmetry in fact have $D_2 \times I^3$ symmetry and (leaving aside the D_{10} pattern) consist of three distinct patterns in one inflation orbit and rotations of these three. In the Penrose tiling case these patterns occur in singular pairs for which appropriate names might be the 'binary star', the 'binary sun' and the 'flip-flop'. The D_2 symmetry makes them ideal for kitchen floor tilings! One is shown in figure 6.

This accounts for all rotations, so all patterns with rotational symmetry are also invariant under reflection as well as under some power of the inflation I.

3.5. Reflection symmetry, subtori and worms

Since the action of complex conjugation on $\mathbb{C} \times \mathbb{C}$ preserves Λ_4 there is a well-defined complex conjugation on $\mathbb{T}^4$ which we denote by $\boldsymbol{t} \to \bar{\boldsymbol{t}}$, and two planar patterns are mirror images in the real axis if and only if their parameters on $\mathbb{T}^4$ are complex conjugates.

The 2D subspace $\mathbb{R} \times \mathbb{R}$ of $\mathbb{C} \times \mathbb{C}$ meets Λ_4 in the 2D lattice $\Lambda_2 = \{(\alpha, \alpha') | \alpha \in \mathbb{Z}[\tau]\}$. Consequently, in the reduction of $\mathbb{C}^2$ to $\mathbb{T}^4 = \mathbb{C}^2/\Lambda_4$, $\mathbb{R} \times \mathbb{R}$ maps to the subtorus $\mathbb{T}^2 = \mathbb{R}^2/\Lambda_2$.

Since points in $\mathbb{T}^2$ are fixed under complex conjugation we have an entire subtorus of patterns with reflection symmetry in the real axis. Moreover, these are the only points on $\mathbb{T}^4$ fixed by complex conjugation: if $\boldsymbol{t} = (z, w)$ and $\bar{\boldsymbol{t}} = \boldsymbol{t}$ then $2(\mathrm{Im}(z), \mathrm{Im}(w)) \in \Lambda_4$, but every purely imaginary $\alpha \in \mathbb{Z}[\xi]$ is of the form $2\,\mathrm{Im}(\beta)$ for some $\beta \in \mathbb{Z}[\xi]$ and hence $(z, w) \in \mathbb{R} \times \mathbb{R} \pmod{\Lambda_4}$.

When the parameter $\boldsymbol{t}$ lies in the subtorus, the intersection of the corresponding pattern with the real axis derives from the points of Λ_2. There is a linear map on $\mathbb{R}^2$ taking Λ_2 to the square lattice while simultaneously taking the x-axis to a line of slope τ'. Consequently the centre line of a 2D pattern with reflection symmetry in the real axis is a pattern in a 1D LI-class (differing from the Fibonacci LI-class only in the width of the window) and there is a one-to-one correspondence between 2D reflection symmetric patterns and the patterns of this LI-class (which represent the well known infinite 'worms' of certain Penrose tilings). Put another way, each infinite worm extends uniquely to a pattern of the 2D LI-class with reflection symmetry in the real axis. Furthermore, an inflation on the 2D LI-class which commutes with reflection restricts to an inflation on the 1D LI-class.

There is a behavioural difference between the RD and TTT LI-classes: because the real axis is the only horizontal line to meet the decagonal window for the RD class in an interval of length 2, infinite worms occur in RD patterns only as axes of reflection symmetry; in TTT patterns, by contrast, every pattern contains lines in the 1D LI-class that reflection axes belong to [3].

The treatment of reflection symmetry in the imaginary axis is similar: again there is a single 2D subtorus (invariant under the negative of complex conjugation) of patterns with this symmetry and the patterns on the reflection axes form a 1D LI-class. This time the behaviour of the RD and TTT classes is reversed: for the TTT class there is a 1D LI-class that occurs only in reflection axes, but for the RD class the 1D LI-class of the reflection axes occurs in all patterns, reflection symmetric or not.

More generally, the operator obtained by combining complex conjugation with multiplication by $(-\xi)^k$ corresponds to the reflection symmetry $R^k S$. The patterns with this symmetry also form a single 2D subtorus, which we denote by $\mathbb{T}^2(k)$. Of the 10 subtori obtained in this way those with even k are, like the subtorus $\mathbb{T}^2(0)$, invariant under complex conjugation and those with odd k are, like the subtorus $\mathbb{T}^2(5)$, invariant under negative complex conjugation. The 10 subtori are cyclically permuted by the action of $-\xi$.

From what we already know of symmetric patterns in the 2D LI-classes we can describe the intersection properties of these subtori as follows.

(1) All the subtori have a common point, corresponding to the pattern with D_{10} symmetry,

(2) $\mathbb{T}^2(1)$, $\mathbb{T}^2(3)$, $\mathbb{T}^2(5)$, $\mathbb{T}^2(7)$ and $\mathbb{T}^2(9)$ have five points in common, corresponding to the single pattern with D_{10} symmetry and the four patterns with D_5 symmetry,

(3) $\mathbb{T}^2(k)$ and $\mathbb{T}^2(k+5)$ meet at four points, corresponding to the pattern with D_{10} symmetry and three patterns (for each $0 \leqslant k \leqslant 4$) with D_2 symmetry forming an inflation orbit.

(4) All intersections of subtori are included among the foregoing.

It is now possible to count how many inflation orbits of length n consist of patterns with reflection symmetry. This number is $10c_n$ with the c_n of table 2 (namely c_n for each of the 10 subtori corresponding to reflection axes), except for the finite number of cases of patterns with more than one reflection symmetry, which we have already considered in detail. The first inflation orbits to have patterns without reflection symmetry occur at $n = 5$, where there are 20 orbits of patterns with reflection symmetry and four of patterns without.

3.6. Interaction between inflation and point symmetry

Let us briefly look at the action of point symmetries on inflation orbits. A more systematic treatment of a joint classification is given in the appendix.

Since $|D_{10}| = 20$, when the number $c_n^{(2)}$ in table 4 is not divisible by 20 there must be some interaction between inflation orbits and point symmetry. The cases $n = 1$ and $n = 3$ have already been considered in detail.

When $n = 4$ there is one inflation orbit in which the patterns have point symmetry D_5 and extended symmetry $D_5 \times (-I^2)$. Consequently the orbit itself has D_{10} symmetry. The remaining five orbits consist of patterns with point symmetry S and extended symmetry $S \times (-I^2)$, as can be deduced from table 3. These orbits have D_2 symmetry.

When $n = 5$ there are four orbits of patterns that have point symmetry but are invariant under $IR^{\pm 4}$. These are 'spirals' on which the action of inflation is the same as rotation through $\pm 4\pi/5$. For the TTT and RD classes these are the patterns generated by the local inflation centred at the fixed point of the rotation-homothety that maps the large obtuse-angled triangle to the small one on the left half of each diagram in figure 3. (The other three orbits in each case result from the action of D_2 on this one.) Since $N_4[\tau - \xi^{\pm 2}] = 11$ these are the only patterns invariant under $IR^{\pm 4}$ (apart from the cartwheel with $D_{10} \times I$ symmetry). Since $N_4[\tau - \xi] = 1$ there are no patterns with exact IR^2 symmetry. The remaining three orbits with $n = 5$ consist of patterns with S symmetry, as we have already seen.

A similar situation occurs with $n = 10$: there are two orbits of patterns with $IR^{\pm 3}$ symmetry. For the TTT and RD classes these are spirals on which the action of inflation is the same as rotation through $\pm 3\pi/5$. They are generated by the local inflation centred at the fixed point of the rotation-homothety that maps the large acute-angled triangle to the lower small one on the right half of each diagram in figure 3. In each LI-class this orbit and its mirror image comprise the only patterns for which inflation is the same as an order of 10 rotation.

Let us finally mention that, since $\tau^{10} - 1 = 11\tau^5$ and τ^5 is a unit, the $11^4 = 14\,641$ patterns with I^{10} symmetry correspond to the 11-division points of $\mathbb{T}^4$, which are isomorphic to the vector space $\mathbb{F}_{11}^4$ (where $\mathbb{F}_{11}$ is the finite field with 11 elements). This space is spanned by four elements, where we may choose one non-trivial member (i.e. with parameter $\boldsymbol{x} \neq \mathbf{0}$) out of each of the four sets of ten 'spiral' patterns with (IR^k) symmetry (for $k = 3, 4, 6, 7$).

4. Tilings of three-space with icosahedral symmetry

Since the experimental discovery of quasicrystals those with icosahedral symmetry (and embedding dimension six) have attracted most attention [14, 13, 6]. Theoretically, three types are possible [23], called P, F and B, derived from the primitive, face-centred and body-centred six-dimensional (6D) hypercubic lattices, respectively. For each of these types, the three-dimensional (3D) subspaces E and E_{int} are the same. The lattice points can no longer be represented by algebraic numbers as in the planar case (quaternions would be needed) but the following is still true for each of these lattices Λ: if A is a linear operator on $\mathbb{R}^6$ that stabilizes Λ, E and E_{int}, and if d is its determinant on E, then $d \in \mathbb{Z}[\tau]$ and $\det A = N_2[d]$. Among such operators, for each of the three types, are those that induce on E all symmetries of the icosahedron. For the fcc and bcc lattices there is also an operator M of this kind that has E and E_{int} as eigenspaces with eigenvalues τ and τ', giving rise to an inflation with the multiplier τ. It is well known, however, that M^3 is the smallest power of M to stabilize the primitive lattice, $\mathbb{Z}^6$. Hence the inflation group of P-type icosahedral quasicrystals is generated by τ^3-inflation.

4.1. Counting inflation orbits

The F- and B-type icosahedral quasicrystals have an inflation with the multiplier τ and the number of patterns of such an LI-class invariant under n-fold inflation is given by

$$a_n^{(3)} = N_2[(\tau - 1)^2] = a_n^3. \tag{40}$$

The corresponding numbers, $b_n^{(3)}$, and orbit counts, $c_n^{(3)}$, are given in table 5. The ζ-function of this inflation operator is

$$Z_3(x) = \frac{(1 - 3x + x^2)^3(1 + 3x + x^2)^3(1 - x^2)^{10}}{(1 - 4x - x^2)(1 - x - x^2)^6(1 + x - x^2)^9} \tag{41}$$

with a functional equation and Riemann hypothesis as for $Z_1(x)$.

Examples of F-type quasicrystals are the Socolar–Steinhardt tiling [26] and Danzer's tiling [6], which belong to the same MLD-class (see [24, 8]). For these the inflation with $\boldsymbol{c} = \mathbf{0}$ is local. There are also B-type quasicrystals with local inflation, but, to our knowledge, only preliminary investigations [19] exist.

For an LI-class of P-type quasicrystals the minimum inflation multiplier is τ^3, and the number of patterns invariant under n iterations of such an inflation is

$$\hat{a}_n^{(3)} = a_{3n}^{(3)} = (a_{3n})^3. \tag{42}$$

Table 5. Inflation orbits of Danzer's tiling (F-type) and other 3D cut-and-project patterns with τ-inflation.

n	1	2	3	4	5	6	7	8	9	10
a_n^3	1	1	64	125	1331	4096	24 389	91 125	438 976	1 771 561
$b_n^{(3)}$	1	0	63	124	1330	4032	24 388	91 000	438 912	1 770 230
$c_n^{(3)}$	1	0	21	31	266	672	3 484	11 375	48 768	177 023

Table 6. Inflation orbit counts of the Kramer–Neri tiling (P-type) and other 3D cut-and-project patterns with τ^3-inflation.

n	1	2	3	4	5
a_{3n}^3	64	4096	438 976	32 768 000	2 537 716 544
$\hat{b}_n^{(3)}$	64	4032	438 912	32 763 904	2 537 716 480
$\hat{c}_n^{(3)}$	64	2016	146 304	8 190 976	507 543 296

The corresponding numbers, $\hat{b}_n^{(3)}$ and $\hat{c}_n^{(3)}$, are given in table 6 (which is, of course, also applicable to iterates of the τ^3-inflation operator on F- and B-type quasicrystals).

The ζ-function of the τ^3-inflation operator on $\mathbb{T}^6$ is

$$\hat{Z}_3(x) = \frac{(1-18x+x^2)^3(1+18x+x^2)^3(1-x^2)^{10}}{(1-76x-x^2)(1-4x-x^2)^6(1+4x-x^2)^9} \tag{43}$$

with the functional equation and Riemann hypothesis as for $Z_1(x)$.

An example of a P-type quasicrystal is the so-called primitive rhombohedral tiling first described by Kramer and Neri [14]. Its τ^3-inflation with $\boldsymbol{c} = \mathbf{0}$ is local [16].

4.2. Cyclic symmetries with one fixed point

In principle, it is a straightforward exercise to determine the Wyckoff positions, which—through the torus parametrization—also determine the patterns with special symmetries. This can be done by standard program packages (adapted to the non-crystallographic symmetries), which will be available soon [9]. In what follows, however, we derive the symmetry structure explicitly by simple arguments and unravel the relation between the various subgroups of Y_h.

The simplest point symmetries to deal with are those which fix only the origin and hence do not have 1 as an eigenvalue. For these the simplest version of our fundamental fact applies.

4.2.1. Inversion symmetry (S_2). To count the patterns in an LI-class invariant under $-\mathbb{1}$ we note that $\det(-\mathbb{1}-\mathbb{1}) = -8$. So the number of patterns with inversion symmetry is

$$|N_2[(-8)]| = 64. \tag{44}$$

As explained in a footnote earlier, these patterns correspond to the two-division points of $\mathbb{T}^6$ and are precisely the 64 patterns invariant under τ^3-inflation.

4.2.2. The S_{10} subgroups. There are six of these subgroups (one for each fivefold-axis of the icosahedron) and each is cyclic of the order of 10 and generated by $-R_5$, where R_5 is

a rotation through $2\pi/5$. Now

$$\det(-R_5 - \mathbb{1}) = -4(\cos(2\pi/5) + 1) = -2\tau^2 \tag{45}$$

so the number of patterns invariant under each S_{10} subgroup is $|N_2[-2\tau^2]| = 4$.

4.2.3. The S_6 subgroups. There are ten of these (one for each threefold-axis of the icosahedron) each generated by $-R_3$, where R_3 is a rotation through $2\pi/3$. The number of patterns invariant under each S_6 subgroup is

$$|N_2[\det(-R_3 - \mathbb{1})]| = |N_2[-4(\cos(2\pi/3) + 1]| = 4. \tag{46}$$

4.3. Mirror symmetries

Let S be one of the 15 mirror symmetries of the icosahedral group and choose an orthonormal basis of E so that the (x, y) plane is the mirror plane. With respect to this basis (and the corresponding orthonormal basis of $E_{\rm int}$) $\mathbb{Z}^3 \oplus \mathbb{Z}^3$ is a lattice in $\mathbb{R}^6$ and the indices of the bcc, primitive and fcc lattices in this are 4, 8 and 16 respectively (see [23]). Taking $A = S - \mathbb{1}$ in the subtorus version of the fundamental fact† (see the appendix) we see that the index of $\Lambda_{\rm ker}$ in $\mathbb{Z}^2 \oplus \mathbb{Z}^2$ is 4, 8 and 16 in the bcc, primitive and fcc cases respectively, and that the index of $\Lambda_{\rm im}$ in $\mathbb{Z} \oplus \mathbb{Z}$ is 4 in all cases. Hence, the index g of $\Lambda_{\rm im} \oplus \Lambda_{\rm ker}$ in Λ is 4 in all three cases. On $\operatorname{im} A = \mathbb{R} \oplus \mathbb{R}$ the action of S is inversion, so the determinant, d, of the restriction of S to $\operatorname{im} A$ is 4. Hence, for all three types of icosahedral quasicrystals each LI-class has a single 4D subtorus of patterns possessing mirror symmetry S.

For each of the 15 mirror symmetries of the icosahedral group there is exactly one 4D subtorus of patterns with that symmetry.

Each such subtorus is stable under inversion, so the fundamental fact shows that it contains exactly 16 inversion symmetric patterns. These patterns are invariant under the group C_{2h} (of order 4) generated by inversion and the mirror symmetry. As we shall see, all these patterns actually have a larger symmetry than C_{2h}.

4.4. Rotation symmetry

If R_2 is the rotation of order 2 about the z-axis then $\operatorname{im}(R_2 - \mathbb{1}) = \ker(S - \mathbb{1})$ and $\ker(R_2 - \mathbb{1}) = \operatorname{im}(S - \mathbb{1})$. Hence the index of $\Lambda_{\rm im} \oplus \Lambda_{\rm ker}$ in Λ is 4 for all three 6D lattices. The action of R_2 on $\operatorname{im}(R_2 - \mathbb{1})$ is inversion, so the determinant of the restriction of R_2 to $\operatorname{im}(R_2 - \mathbb{1})$ is 16 and there are four 2D subtori of patterns with a 2nd order rotation symmetry about the z-axis.

Rotations R of order 5 and 3 can be treated similarly. The index of $\Lambda_{\rm im} \oplus \Lambda_{\rm ker}$ in Λ is 5 for order 5 rotations and 9 for order 3, and these indices are the same for all three 6D lattices Λ. Since $N_2[\det(R - \mathbb{1})]$ is 5 when R has order 5 and 9 when R has order 3, for each fivefold and threefold rotation axis there is just one 2D subtorus of patterns with that rotation symmetry. Since this subtorus contains $\{\mathbf{0}\}$ it lies entirely in the subtorus of those mirror symmetries that contain the rotation axis in their mirror plane. Hence, all patterns with C_5 or C_3 symmetry also have C_{5v} or C_{3v} symmetry.

For each of the six fivefold rotation axes there is exactly one 2D subtorus of patterns with the corresponding C_5 rotation symmetry. A generic pattern on the subtorus has symmetry group C_{5v}.

† For simplicity of notation, in this section the same symbol will be used to denote a symmetry of the icosahedron and the lift of the symmetry to $\mathbb{R}^6$.

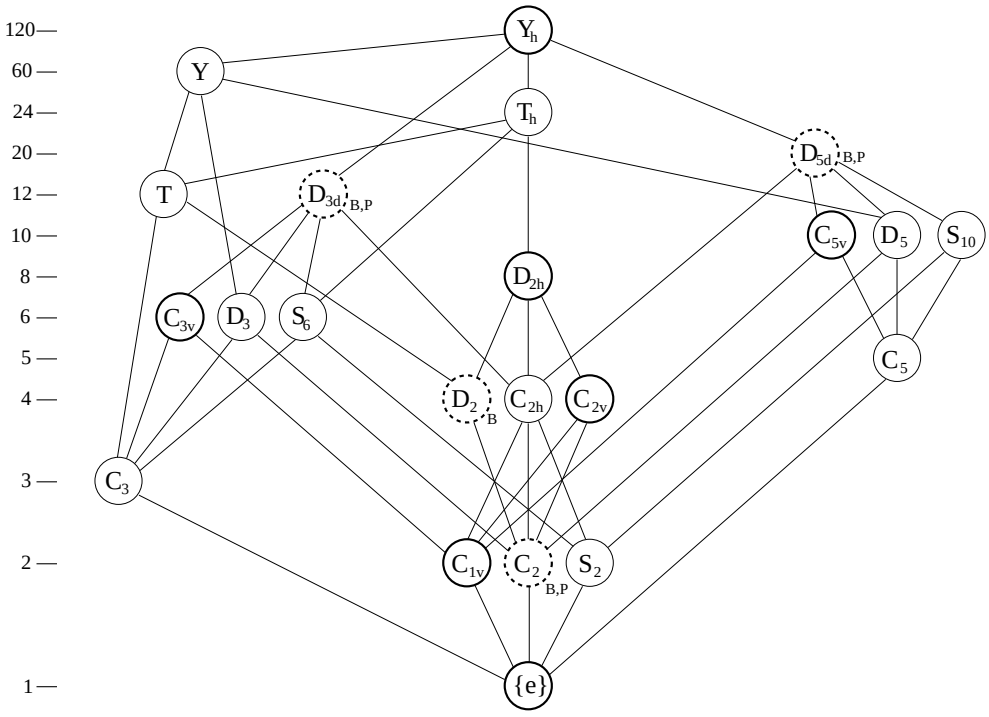

Figure 7. Conjugacy classes of subgroups of the icosahedral group. Heavy circles indicate that the corresponding group appears in all three cases as a maximal symmetry of some pattern, while groups with broken circles appear only for patterns of B- or P-type. Finally, the groups $\{e\}$, C_{1v}, C_2, C_{2v}, C_{3v} and C_{5v} admit entire subtori of solutions.

For each of the ten threefold rotation axes there is exactly one 2D subtorus of patterns with the corresponding C_3 rotation symmetry. A generic pattern on the subtorus has symmetry group C_{3v}.

As a consequence of this, and by inspection of the diagram of subgroups in figure 7, it is clear that the four S_{10}-symmetric patterns for each fivefold axis are automatically also D_{5d}-symmetric and the S_6-symmetric patterns are also D_{3d}-symmetric. Note that this also means that there are no patterns with the tetrahedral groups, T, nor $T_h = T \times S_2$, the icosahedral group, Y, nor the group D_3 as their maximal symmetry since all these groups contain C_3 but not C_{3v} as a subgroup. Similarly, there is no pattern with D_5 as its full symmetry.

4.5. Patterns with full icosahedral symmetry Y_h

So far, we have obtained the total numbers of patterns with D_{3d} or D_{5d} symmetry (for a given axis). It remains to determine which of those patterns have an even larger symmetry group. As can be seen from figure 7, this larger symmetry group can only be the full icosahedral group Y_h and a pattern is Y_h-symmetric if and only if it is simultaneously D_{3d}- and D_{5d}-symmetric.

For further analysis we need an explicit determination of the symmetry solutions on the torus. There is no loss of generality in taking the threefold-axis to be $(\tau^2, 1, 0)$ and the fivefold-axis to be one of $(1, \pm\tau, 0)$. Let us take just the fcc case as an example. The

Table 7. Point symmetries of the 64 inversion symmetric tilings for the three different icosahedral types.

Group	B-type	P-type	F-type
Y_h	1	2	4
D_{5d}	18	12	0
D_{3d}	30	20	0
D_{2h}	15	30	60

lattice projects to the submodule $\mathcal{M}_F$ of $\mathbb{Z}[\tau]^3$ in $\mathbb{R}^3$ defined by

$$\begin{aligned} &\tau^2 x + \tau y + z \equiv 0 \pmod 2 \\ &x + y + z \equiv 0 \pmod 2 \end{aligned} \tag{47}$$

see [4]. (In $\mathbb{Z}[\tau]$ there are four residue classes mod 2 with representatives 0, 1, τ, τ^2.) The intersection of this module with $\mathbb{R}^2$ is $(2\mathbb{Z}[\tau])^2$ so the four two-division points on the D_{3d} subtorus project to the multiples of $(\tau^2, 1, 0)$ by 0, 1, τ, and τ^2 and the four two-division points on the D_{5d} subtorus project to the multiples of $(1, \pm\tau, 0)$ by 0, 1, τ, and τ^2. But

$$\tau(\tau^2, 1, 0) \equiv (1, \pm\tau, 0) \pmod 2 \tag{48}$$

so the corresponding points are identical on the torus. The multiples of these points are similarly identified, so each D_{3d}-symmetric pattern is also D_{5d}-symmetric in this case.

This way, we find one pattern with full Y_h symmetry for the bcc lattice, two for the primitive lattice and four for the fcc lattice.

We are now in a position to classify all patterns with inversion symmetry. Let y_h be the number of patterns with Y_h symmetry. Then for each of the six fivefold-axes there are $4-y_h$ patterns whose full symmetry is D_{5d} and for each of the ten threefold-axes there are $4-y_h$ patterns whose full symmetry is D_{3d}. So the total number of patterns of symmetry types Y_h, D_{5d} and D_{3d} is $y_h + 16(4-y_h) = 64 - 15y_h$. Of the 16 patterns with C_{2h} symmetry for a given twofold-axis, y_h have full symmetry Y_h, $2(4-y_h)$ have full symmetry D_{5d} and $2(4-y_h)$ have full symmetry D_{3d} (since there are two fivefold and two threefold-axes perpendicular to the twofold-axis) accounting for $16-3y_h$ patterns in all. Let c_{2h} and d_{2h} be the number with full symmetry C_{2h} and D_{2h} respectively. Then

$$c_{2h} + d_{2h} = 3y_h. \tag{49}$$

The patterns with full symmetry C_{2h} have a single twofold axis but those with D_{2h} symmetry have three mutually perpendicular twofold axes. Since these patterns have inversion symmetry and there are 64 inversion-symmetric patterns altogether, we have

$$15c_{2h} + 5d_{2h} \leqslant 15y_h. \tag{50}$$

Together with (49) this gives $c_{2h} = 0$ and $d_{2h} = 3y_h$. Since there is equality in (50) the symmetry types of all patterns with inversion symmetry are now accounted for. In particular, all 16 C_{2h}-symmetric patterns for each twofold axis are also at least D_{2h}-symmetric.

Table 7 summarizes these results giving, for each type of lattice, the total number of patterns of each symmetry type in an LI-class.

We have now accounted for all subgroups with only one fixed point except those of type D_2.

The different symmetry counts from the different lattice types show that no two icosahedral cut-and-project patterns obtained from different lattice types are mutually locally derivable.

All inversion symmetric patterns are invariant under simple τ^3-inflation for the P-type. The fact that there are two Y_h-symmetric patterns when the primitive lattice is used confirms that this lattice has no inflation operator with multiplier τ, as τ-inflation has only one orbit of length 1 and no orbits of length 2.

For B- and F-type, one of the icosahedral patterns is invariant under τ-inflation. The other inversion symmetric patterns form three-cycles under inflation. Furthermore, for each rotation axis or mirror plane of the icosahedron separately, the inflation orbits preserve the point symmetry of the corresponding patterns.

4.6. Subgroups containing a rotation of the order of 2

As mentioned above, we have, for each rotation axis of the order of 2, precisely four disjoint 2D subtori of C_2-symmetric patterns. To complete our classification, we need to know whether these patterns are also mirror symmetric (such as the cases with threefold and fivefold rotational symmetry). As for the icosahedral symmetry, an explicit determination of the symmetry solutions (representing symmetric patterns) is needed—we only give the results here.

It turns out that for B-, P- and F-type there are one, two and four subtori, respectively, that lie entirely within the 4D subtori of those mirror reflections that fix the rotation axis under consideration. Consequently, the patterns on these subtori are at least C_{2v}-symmetric. Since all possible higher symmetries also contain space inversion, the corresponding patterns have already been classified. In fact, each C_{2v}-subtorus contains exactly one solution with full icosahedral symmetry.

We can now conclude that there are no patterns with C_2 or D_2 as maximal symmetry in the F case, but we must have C_2-symmetric ones for bcc and primitive lattices (no proper supergroup of C_2 except C_{2v} admits an entire subtorus of solutions, compare with figure 7). Finally, an explicit check shows that there are no D_2-symmetric patterns for the P-type, but 12 of them for each twofold-axis when the bcc lattice is used. So in this case we get another 60 isolated solutions to a subgroup with only one fixed point. They form orbits of length 6 under inflation.

With this, the classification of the possible geometric symmetry subgroups is complete, and we have indicated, while working through the various cases, how the symmetric patterns group into inflation orbits.

5. Concluding remarks

The torus parametrization of cut-and-project patterns has been introduced in order to illuminate the stucture of the corresponding local isomorphism classes, in particular to investigate patterns of special symmetry, either ordinary point or more general inflation symmetry. The concept was illustrated by various examples of tilings in dimensions less than or equal to three with τ- or τ^3-inflation. Clearly, the method can be applied to other cases of physical interest, such as planar quasicrystals with eightfold or twelvefold symmetry [11], and also to higher-dimensional cases such as the Elser–Sloane 4D quasicrystal based on the root lattice E_8. The results will be reported separately.

In this article, it was our aim to set the scene and to explain, for the most important examples, what the general structure is and which of the aspects are universal. It is perhaps rather surprising that these results largely depend only on the eigenvalues of the operators. There is more variability between LI-classes (or, more precisely, S-MLD-classes [5]), however, in the way symmetries distribute over regular and singular patterns, which

depends on the size, shape and orientation of the window as well as on the lattice. This is certainly worth further investigation, though some topological constraints are obvious from recent considerations [15].

Although the picture of quasiperiodic LI-classes looks quite promising in this light, much less is known about other cases, even in one dimension. Many prominent examples, such as the Thue–Morse chain, can be partially dealt with individually, but at the moment we do not know of any general method to treat them in a similar fashion to the quasiperiodic cases. It would be interesting to see some unified results, perhaps for a substantial subclass with sufficiently amiable properties such as closure and strict ergodicity under translations.

Acknowledgments

It is a pleasure to thank Franz Gähler for helpful discussions and Martin Schlottmann for various comments on the manuscript. This work was supported by the German Science Foundation (DFG).

Appendix. General structure of the torus parametrization

Let us now consider, in a more general fashion, the situation of a discrete pattern (a tiling or point set with certain point and inflation symmetries) that is obtained from a higher-dimensional periodic structure by the projection method. This means that we consider an LI-class which is closed under the action of these symmetries and which is quasiperiodic in the sense that the diffraction image consists of Bragg peaks only. Right from the start, we have a lattice embedding at our disposal where all symmetries are represented by lattice endomorphisms (i.e. integer matrices with respect to the lattice basis), or by affine extensions of that. The entire space spanned by our lattice, Λ, is the direct sum of some space E which carries the tiling (often called *physical* or *tiling* space) and some space E_{int} (the *internal* space). Both are invariant under the action of all of our symmetries under consideration.

We further assume that the embedding is minimal (hence the lattice, Λ, projects densely into E_{int}) and that the origin is the only point in $E \cap \Lambda$ (which is a kind of irrationality assumption). This is actually no restriction, but simplifies the discussion considerably. Also, we only consider structures that are described by an admissible window system, W, which is compatible with our symmetries, in other words for which there is always at least one (possibly singular) pattern of maximal symmetry, and this is, in our setting, the one parametrized by the trivial solution $\boldsymbol{t} = \mathbf{0}$. Finally, we assume that the boundary, ∂W, of the windows is of the measure 0, as otherwise several unphysical features can arise, including a deviation from quasiperiodicity as defined above.

Our tiling defines an LI-class which can be parametrized by the points of one fundamental domain of the lattice Λ which is, after proper identification of translationally equivalent boundaries, an n-dimensional torus, $\mathbb{T}^n$ (with n being the rank of Λ). A point $\boldsymbol{t}$ of $\mathbb{T}^n$ either corresponds uniquely to one *regular* tiling (iff $\boldsymbol{t}$ is not in the set $\partial W + \pi_{\mathrm{int}}(\Lambda)$) or to a finite† number of *singular* tilings which are identified in this picture (they differ only in mismatches of density 0, such as points on lower-dimensional manifolds). With this

† If the window is not a polytope, but more complicated such as fractally shaped, it might occur that one identifies infinitely many tilings here. However, as long as ∂W has measure 0, the (singular) tilings of the LI-class identified cannot differ in mismatches of positive density. (This statement follows from various results, in particular [25, section 2.2.3].) Furthermore, regular tilings are still generic in the LI-class.

identification, one can now determine tilings with special symmetries by solving appropriate equations on the torus!

A.1. Symmetry analysis and proof of the fundamental fact

A generalized symmetry is given by a mapping, $\mathbb{T}^n \to \mathbb{T}^n$, of the form

$$\boldsymbol{t} \mapsto A\boldsymbol{t} + \boldsymbol{c} \bmod \mathbb{T}^n \tag{A.1}$$

where $\boldsymbol{c} \in \mathbb{T}^n$ and A is an integer matrix in the torus basis. (For geometric point symmetries, we actually have $\boldsymbol{c} = \boldsymbol{0}$ due to our standardization.) Tilings with such a symmetry are just those parametrized by fixed points of (A.1) on $\mathbb{T}^n$ and hence solve the equation

$$(A - \mathbb{1})\boldsymbol{t} + \boldsymbol{c} = \boldsymbol{0} \bmod \mathbb{T}^n. \tag{A.2}$$

The fundamental fact states that there are precisely

$$k = |\det(A - \mathbb{1})| \tag{A.3}$$

isolated solutions. They are the only ones if $(A - \mathbb{1})$ is *regular*, i.e. if $k \neq 0$. If, however, $(A - \mathbb{1})$ is *singular*, the solutions are never isolated, but fill entire subtori. Let us now formulate the underlying structure together with a proof.

Fundamental fact (point version). Let Λ be a lattice in $\mathbb{R}^n$ and A a non-singular linear operator on $\mathbb{R}^n$ with $A\Lambda \subseteq \Lambda$. (Hence A acts on a fundamental region of Λ, which is an n-dimensional torus $\mathbb{T}^n = \mathbb{R}^n/\Lambda$.) Take any $\boldsymbol{c} \in \mathbb{T}^n$. Then the number of points $\boldsymbol{t} \in \mathbb{T}^n$ with

$$A\boldsymbol{t} = \boldsymbol{c} \tag{A.4}$$

is $d = |\det A|$.

Proof. $A\boldsymbol{t} = \boldsymbol{c}$ on $\mathbb{T}^n$ if and only if $\boldsymbol{t} = \boldsymbol{u} + A^{-1}\boldsymbol{c}$, where $A\boldsymbol{u} \in \Lambda$, so we need to count the number of solutions, $\boldsymbol{u}$, to $A\boldsymbol{u} \in \Lambda$ that are distinct mod Λ. Clearly $A^{-1}\Lambda \supseteq \Lambda$ and the index is d, so this number of solutions is d. □

Fundamental fact (subtorus version). Let Λ be a lattice in $\mathbb{R}^n$ and A a diagonalizable linear operator on $\mathbb{R}^n$ with $A\Lambda \subseteq \Lambda$. Put $s = \dim(\ker A)$, $\Lambda_{\ker} = \Lambda \cap \ker A$ and $\Lambda_{\mathrm{im}} = \Lambda \cap \mathrm{im}\, A$ and let g be the index of $\Lambda_{\mathrm{im}} \oplus \Lambda_{\ker}$ in Λ and d the determinant of the restriction of A to $\mathrm{im}\, A$. Then the points $\boldsymbol{t} \in \mathbb{T}^n$ with

$$A\boldsymbol{t} = \boldsymbol{0} \tag{A.5}$$

comprise d/g s-dimensional subtori of $\mathbb{T}^n$ which are translates of each other.

Proof. Since A is diagonalizable, we have $\mathrm{im}\, A \oplus \ker A = \mathbb{R}^n$, and since $A\Lambda \subseteq \Lambda$, Λ_{im} and $\Lambda_{\ker}$ are lattices of full dimension in $\mathrm{im}\, A$ and $\ker A$, respectively. Every $\boldsymbol{x} \in \mathbb{R}^n$ can be written as $\boldsymbol{x} = \boldsymbol{y} + \boldsymbol{z}$, with $\boldsymbol{y} \in \mathrm{im}\, A$ and $\boldsymbol{z} \in \ker A$, and $A\boldsymbol{x} \in \Lambda$ if and only if $A'\boldsymbol{y} \in \Lambda_{\mathrm{im}}$, where A' is the restriction of A to $\mathrm{im}\, A$ and is non-singular since $\mathrm{im}\, A \cap \ker A = \{\boldsymbol{0}\}$. By the point version of the fundamental fact there are d points $\boldsymbol{y}_1, \ldots, \boldsymbol{y}_d$ in $\mathrm{im}\, A$ (distinct mod Λ) with $A'\boldsymbol{y}_i \in \Lambda_{\mathrm{im}}$. Hence, the solutions of $A\boldsymbol{x} \in \Lambda$ are

$$\boldsymbol{x} = \boldsymbol{y}_i + \boldsymbol{z} \qquad (i = 1, \ldots, d,\ \boldsymbol{z} \in \ker A) \tag{A.6}$$

which reduce mod Λ to the subtori of $\mathbb{T}^n$

$$\mathbb{T}(\boldsymbol{y}_i) = \boldsymbol{y}_i + (\ker A/\Lambda_{\ker}) \qquad (i = 1, \ldots, d). \tag{A.7}$$

Let $\boldsymbol{u}_1 + \boldsymbol{v}_1, \ldots, \boldsymbol{u}_g + \boldsymbol{v}_g$ ($\boldsymbol{u}_i \in \mathrm{im}\, A$, $\boldsymbol{v}_i \in \ker A$) be a set of coset representatives of $\Lambda_{\mathrm{im}} \oplus \Lambda_{\ker}$ in Λ. Then $\boldsymbol{u}_1, \ldots, \boldsymbol{u}_g$ are distinct mod Λ_{im} and $\mathbb{T}(\boldsymbol{y}_i) = \mathbb{T}(\boldsymbol{y}_j)$ if and only

if $\boldsymbol{y}_i - \boldsymbol{y}_j \equiv \boldsymbol{u}_k \pmod{\Lambda_{\mathrm{im}}}$ for some k. So subtori (A.6) are equal in sets of g. Hence, the points, $\boldsymbol{t}$, on $\mathbb{T}^n$ with $A\boldsymbol{t} = \boldsymbol{0}$ consist of d/g translates of the s-dimensional subtorus $\ker A/\Lambda_{\mathrm{ker}}$. □

A.2. The structure of the symmetry solutions on $\mathbb{T}^n$

Let $\boldsymbol{c} = \boldsymbol{0}$. Then (A.2) is a homogeneous equation, so the superposition principle guarantees that the set of solutions has an important additional structure: it forms an Abelian subgroup of $\mathbb{T}^n$. This will be helpful later. For any finite shift $\boldsymbol{c}$, the general solution is obtained from one particular solution of the inhomogeneous case plus any solution of the linear case.

Let now $(A - \mathbb{1})$ be non-singular. If we consider a special solution $\boldsymbol{t}_0$ of (A.1), it generates (since $\boldsymbol{c} = \boldsymbol{0}$) an additive subgroup of $\mathbb{T}^n$ of solutions which must be of the finite order of k. Written in the torus basis, every solution $\boldsymbol{t}_0$ takes the following standard form:

$$\boldsymbol{t}_0 = \frac{1}{m}(l_1, l_2, \ldots, l_n)^t \tag{A.8}$$

with non-negative integers $l_1, l_2, \ldots, l_n$ all smaller than the integer $m \leqslant k$, and $\gcd(m, l_1, l_2, \ldots, l_n) = 1$ (overall coprimality).

On the other hand, now take *any* rational point of the form (A.8). If we now act with an invertible integral matrix, M, of infinite order (which may represent e.g. an inflation, assumed strictly linear for the moment) on such a $\boldsymbol{t}_0$, the image is again a point with rational coordinates with the same m—hence iterated action of M generates a closed orbit on $\mathbb{T}^n$. This means: *every* rational point on $\mathbb{T}^n$ is a solution to a certain symmetry (at least to a higher inflation), and they are obviously the only ones. The tilings with special symmetries correspond to rational points on $\mathbb{T}^n$, which are of the measure 0, but dense. Furthermore, they can have a rather complicated relation to the set of singular points (which are also of the measure 0 and dense).

A.3. Joint classification of point and inflation symmetries

One standard situation is that the inflation M acts on E and E_{int} just as a multiplication. In this case, M commutes with S for all point symmetries, S, of the tiling and symmetry is preserved on inflation orbits, i.e. all members of one inflation orbit share the same point symmetry (if any). This observation has been used above to predict simultaneous point and inflation symmetries, even if only the total number of solutions in each case is known.

For the more general case, we have to consider the inflation to be *affine*:

$$\boldsymbol{t} \mapsto M\boldsymbol{t} + \boldsymbol{c} \tag{A.9}$$

where, with $\boldsymbol{a} := -M\boldsymbol{c}$, $\boldsymbol{c}$ can also be expressed as $\boldsymbol{c} = \boldsymbol{a} - M\boldsymbol{a}$. The fixed points of this transformation are clearly those of the linear transformation M, shifted by $\boldsymbol{a}$. This indicates a shift of the inflation origin by $\boldsymbol{a}$ on the torus. (For the pattern, it is the part of $\boldsymbol{a}$ parallel to E which fixes the inflation centre relative to the point symmetry centre.) The following cases can be distinguished:

(1) $\boldsymbol{a}$ is rational and a solution for a geometric point symmetry S. Then S still commutes with the inflation and nothing is changed in their joint classification (except possibly the assignment of the special patterns to the inflation orbits).

(2) $\boldsymbol{a}$ is rational, but not a solution for a geometric point symmetry S. All isolated solutions with geometric point symmetry still also possess an inflation symmetry, but inflation orbits no longer preserve symmetry. A joint classification is possible, but less natural.

(3) $\boldsymbol{a}$ is irrational. Isolated solutions for point symmetries never show inflation symmetry.

A.4. Translation classes

While a shift parallel to $E_{\rm int}$ may change the character of the inflation (and in general even affects its locality), a shift in the physical direction simply moves the inflation centre. Since a choice here is somehow arbitrary, it is quite natural to consider elementary translation classes of tilings rather than single tilings themselves. Such classes consist of a special pattern and all its global translates. On the torus, they show up as

$$[\boldsymbol{t}_0] := \{\boldsymbol{t}_0 + \boldsymbol{a} \bmod \mathbb{T}^n | \boldsymbol{a} \in E\}. \tag{A.10}$$

Since $E \cap \Lambda = \{\mathbf{0}\}$ by assumption, there is at most one rational $\boldsymbol{t}$ in $[\boldsymbol{t}_0]$. Consequently, we have a one-to-one relation between elements of the LI-class with special point or rescaling symmetries and their elementary translation classes if it is a situation with *finitely* many solutions. The torus parametrization can thus be used equally as well to classify translation classes. A bit more care is needed in situations with continuous manifolds of solutions, but we do not go into detail here.

References

[1] Baake M and Joseph D 1990 Ideal and defective vertex configurations in the planar octagonal quasilattice *Phys. Rev.* B **42** 8091–102

[2] Baake M, Joseph D and Schlottmann M 1991 The root lattice D_4 and planar quasilattices with octagonal and dodecagonal symmetry *Int. J. Mod. Phys.* B **5** 1927–53

[3] Baake M, Kramer P, Schlottmann M and Zeidler D 1990 Planar patterns with fivefold symmetry as sections of periodic structures in 4-space *Int. J. Mod. Phys.* B **4** 2217–68

[4] Baake M and Pleasants P A B 1995 Algebraic solution of the coincidence problem in two and three dimensions *Z. Naturf.* **50a** 711–17

[5] Baake M and Schlottmann M 1995 Geometric aspects of tilings and equivalence concepts *Proc. 5th Int. Conf. on Quasicrystals* ed C Janot and R Mosseri (Singapore: World Scientific) pp 15–21

[6] Danzer L 1989 Three-dimensional analogs of the planar Penrose tilings and quasicrystals *Discrete Math.* **76** 1–7

[7] Danzer L and Dolbilin N 1997 On Delone-graphs and the number of congruence-classes in certain species of such graphs *The Mathematics of Aperiodic Order* ed R V Moody (Dordrecht: Kluwer) in press

[8] Danzer L, Papadopolos Z and Talis A 1993 Full equivalence between Socolar's tilings and the (A, B, C, K)-tilings leading to a rather natural decoration *Int. J. Mod. Phys.* B **7** 1379–86

[9] Gähler F 1996 Private communication

[10] Hardy G H and Wright E M 1979 *An Introduction to the Theory of Numbers* 5th edn (Oxford: Clarendon)

[11] Hermisson J, Richard C and Baake M 1996 A guide to the symmetry structure of quasiperiodic tiling classes *Preprint* Tübingen

[12] Janssen T 1988 Aperiodic crystals: a contradictio in terminis? *Phys. Rep.* **168** 55–113

[13] Katz A and Duneau M 1986 Quasiperiodic patterns and icosahedral symmetry *J. Physique* **47** 181–96

[14] Kramer P and Neri R 1984 On periodic and non-periodic space fillings of E^m obtained by projection *Acta Crystallogr.* A **40** 580–7

Kramer P and Neri R 1985 *Acta Crystallogr.* A **41** 619 (erratum)

[15] Le T Q T 1997 Local rules for quasiperiodic tilings *The Mathematics of Aperiodic Order* ed R V Moody (Dordrecht: Kluwer) in press

[16] Lück R 1992 Private communication

[17] Lunnon F and Pleasants P A B 1987 Quasicrystallographic tilings *J. Math. Pure Appl.* **66** 217–63

[18] Niizeki K 1989 A classification of special points of quasilattices in two dimensions *J. Phys. A: Math. Gen.* **22** 4281–93

Niizeki K 1989 A classification of special points of icosahedral quasilattices *J. Phys. A: Math. Gen.* **22** 4295–302

[19] Papadopolos Z, Baake M, Klitzing R and Kramer P 1993 From the weight lattice D_6^R to icosahedral tilings *Proc. 3rd Int. Wigner Symposium (Oxford)* ed M Angelova, L L Boyle and A I Solomon (Singapore: World Scientific) in press

[20] Parry W and Pollicott M 1990 Zeta functions and the periodic orbit structure of hyperbolic dynamics *Astérisque* **187–188** 1–268

[21] Pleasants P A B 1985 Quasicrystallography: some interesting new patterns *Elementary and analytic theory of numbers* (Warsaw: PWN) pp 439–61

[22] Pleasants P A B 1995 Quasicrystals with arbitrary symmetry group *Proc. 5th Int. Conf. on Quasicrystals* ed C Janot and R Mosseri (Singapore: World Scientific) pp 22–30

[23] Rokhsar D S, Mermin N D and Wright D C 1987 Rudimentary quasicrystallography: The icosahedral and decagonal reciprocal lattices *Phys. Rev.* B **35** 5487–95

[24] Roth J 1993 The equivalence of two face-centered icosahedral tilings with respect to local derivability *J. Phys. A: Math. Gen.* **26** 1455–61

[25] Schlottmann M 1993 Geometrische Eigenschaften quasiperiodischer Strukturen *Dissertation* University of Tübingen

[26] Socolar J E S and Steinhardt P J 1986 Quasicrystals. II. Unit-cell configurations *Phys. Rev.* B **34** 617–47